Study of Corrosion Behavior of Al_2O_3 and WC−12% Co Coatings Deposited by Plasma Spraying

M. A. H. EL-Meniawi[1] and D. Saber*[1] K. M. Zohdy[2]

[1]Materials Engineering Dept., Faculty of Engineering, Zagazig University, Zagazig, Egypt

Corresponding author: [2] Email: daliasaber13@yahoo.com (D. Saber).

Tel: +2-0106-3970239; Fax: +2-055-2304987

Abstract

In this study the corrosion behavior of coated austenitic steel was investigated using 0.5M H_2SO_4 solutions. Austenitic steel; known traditionally as (PL−1200 R5) was used as substrates. The ceramic coatings using plasma spray process was employed on a substrate with deposition of Al_2O_3 and WC−12% Co using atmospheric plasma spray (APS) equipment with a F4-MB torch by using different parameters and deposition techniques. The porosity of coatings was measured by impregnation method. Potentiodynamic polarization measurements were carried out to determine the corrosion behavior of the plasma-sprayed-coatings. The microstructure of the coatings and corroded coatings were characterized by scanning electron microscopy(SEM) /energy dispersive X-ray spectroscopy(EDX). It is concluded that the corrosion resistance depends strongly on the porosity and the type of coating.

Keywords:

Ceramics; Coatings; plasma deposition ; Porosity; Corrosion.

1. Introduction

Ceramic coating materials are considered optimal in their applications [1–3], when compared to materials-coating, either metallic or organic -which are used under different environmental conditions and exposed to mechanical wear and corrosion particularly at high temperatures. For example, alumina and zirconia coatings are increasingly and widely used for a range of industrial applications to provide wear and erosion resistance, corrosion protection and thermal insulation [4,5]. Alumina ceramic can retain up to 90% of their strength even at 1100^{o}C. Alumina ceramics are widely

used in many applications because of their excellent properties. These applications include: refractory materials, grinding media, cutting tools, high temperature bearings, a wide variety of mechanical parts, and critical components in chemical process environments. Materials which are subjected to aggressive chemical attack, increasingly higher temperatures and pressures fall into this category [6]. Such coatings have small structural defects, e.g., pinholes, pores and microcracks. These local defects are formed during or after spraying and act as channels which cause a direct path between the corrosive environment and substrate, leading to rapid local galvanic attacks and pitting corrosion of the base materials [7–10]. Many factors influence the corrosion characteristics of coatings, including their quality and structure [11,12]. Test technique in 0.5 N H_2SO_4 solution, in addition to the effect of some parameters e.g., porosity, thickness of the coating on corrosion behavior of these coatings were also studied. The porosity is usually used as a parameter of the structure of plasma sprayed coating [13]. In aggressive environments, one of the major problems in using plasma-sprayed coatings is the presence of the open pores, closed pores and micro-cracks in the coatings [14]. Therefore, reduction of porosity of the sprayed coatings plays a key role in improving the corrosion resistance of the coatings. Many studies have contributed to a better understanding of the metallographic preparation, microstructure, thermal conductivity and failure mechanisms of the ceramic coatings [15]. However, the effects of the process parameters on the microstructure and properties of the ceramic coatings have not been fully understood yet. The main aim of this study is to evaluate the corrosion resistance of austentic stainless steel, coated with Al_2O_3, and WC−12%Co using the plasma spray technique.

2. Experimental Technique

2.1. Plasma spray deposition

Substrates used in this study were austenitic steel which is known traditionally as (PL−1200 R5) with the dimensions 25x20x2 mm. The ceramic coatings were carried

out via atmospheric plasma spray (APS) equipment with a F4-MB torch . The powder feed unit supplies the plasma gun with spray powder in a very exact and reproducible manner. The powder feeder has to be able to feed powders of greatly different types from small to very large amounts. The main parts of a plasma burner are a water cooled " cathode " with a tip of thoriated tungsten, and also water cooled nozzle shaped " anode " and an isolating ring keeping both electrodes electrically separated. In the plasma spray process, the spray gun used in some machines is to be fixed in a specified location, meanwhile the pieces to be coated are rotating around the machine spindle in one direction facing the sprayed powder. This motion is continuous until the required coated thickness gained. The proposed work is to change the direction of coating after getting a certain value of thickness. This is very easy to be achieved by changing the fixation of specimens around the axis by 90^{o}. In this case, the next layers of coating are in a direction normal to the previous ones. However, the spraying process occurred in parallel and in traversal paths by using gray aluminum oxide of Metco 101 NSC as coarse grain and AMDRAY 187F fine grain. Also by the same way spraying powder of tungsten carbide (WC) – 12% cobalt (Co) of Metco 71 VFNS as fine grain and AMDRY 301C as coarse grain. Coatings were produced using a plasma spray parameters as presented inTable 1.

2.2. Porosity

As the corrosion reactions are initiated at the coating substrate interface, the measurement of porosity becomes essential for estimating the corrosion resistance of the whole coated component. Water impregnation method was used to determine the porosity applying the relation:

$$W = \{ (M-D)/(M-S) \} \times 100$$

Where:

W is the percentage volume of porosity

M is the weight as saturated in air

D is weight as dry sample

S weight as suspended in water

Thus, flat specimens were cut perpendicular to coated surface and then grounded using emery papers of grades 180, 220, 280, 400, 600, and 1200 respectively. Final polishing was done using 1µm alumina super finish.

2.3. Corrosion test and procedure

Electrochemical tests were conducted in 0.5 M H_2SO_4 solution prepared prior to each test using distilled water. All electrochemical experiments were conducted with a Gamry PCI300/4 Potentiostat / Galvanostat/Zra analyzer, connected to a PC. The Echem Analyst Software (version 5.21) was used for all electrochemical data analysis. A three-electrode-cell was used in these experiments. The electrodes are composed of:-

- A specimen as a working electrode
- Platinum counter electrode
- Saturated calomel electrode (SCE) as a reference electrode

Tafel polarization tests were carried out using a scan rate of 0.5 mV/min at 25 °C. Specimens, with exposed surface area of 1.5 cm^2, were used as a working electrode. Prior to electrochemical tests, the specimens were cathodically cleaned for 15 min at -1500 mV (SCE) to remove the air-formed oxide film. The applied routine automatically selects the data that lies within the Tafel region (±250 mV with respect to the corrosion potential).

2.4. Microstructure

Optical microscopy, Scanning Electron Microscopy (SEM) and Energy-Dispersive X−ray spectroscopy (EDX) were carried out in order to:-

- Identify phases of the samples
- Characterize their morphology and chemical characterization

- Determine key features that contribute to the corrosion.

3. Results and discussion

3.1. Microstructures

The SEM micrographs of plasma-sprayed-coatings (PSC) are given in Fig. (1). It is shown that (PSC) usually exhibit porosity, oxides, un-melted particles and inclusions. The ceramic coatings of perpendicular spray direction denoted by (A for WC−12%Co, B for Al_2O_3) shows more porous structure compared to the parallel coatings denoted by (A1 for WC−12%Co, B1 for Al_2O_3) as shown in Fig.1(a−d). For instance, the WC−12% Co coating exhibits high porosity with large pore sizes and relatively wide distribution. Also WC−12%Co coating exhibits a large number of micropores with a wide pore size distribution as shown in Fig. 1 (a,b). For Al_2O_3 coating, the defects were mainly in the form of micro pores, and no visible micro cracks were found in it as illustrated in Fig.1 (c,d) [16].The pores are caused by the splashing of particles on impact with deposited material. It may be due to voids resulting from the poor deformation of partially melted particles. These pores can have different sizes and exceedingly intricate shapes [17].The presence of pores, cracks, and localized compositional variations could degrade corrosion resistance [18].

However, the SEM micrographs proved less microporoes, cracks and more corrosion resistant for Al_2O_3 coating than WC−12%Co coating. Type of defects that have been detected in our SEM micrographs for WC−12%Co coating are:

1- Cracks were found on the surface of both coated specimens
2- Irregular shape results in the coat layers, hence making the coating more porous .

3-SEM micrograph of WC−12%Co coating Fig.2 surfaces shows more number of pores/voids as compare to the Al_2O_3 coatings Fig. 3 .

3.2. Porosity analysis

The porosity analysis results of coatings produced are summarized in Table 2. All numbers showed in Table (2) represent average percentage of the porosity calculated by using the accurate form of the equation. In the case of Al_2O_3 coatings, porosity can be intra-lamellar. Inter-lamellae pores mostly form from the random build-up of splats and the volume change during solidification results in intra lamellae pores [19]. The optimal composition taking both mechanical stability and high deposition efficiency of coatings increased as expected with an increase of the alumina content from 40- 60 wt% Al_2O_3 [20]. Further, several possible sources of porosity in a coating have also been identified including:

- Curling up of splats due to thermal stresses
- Incomplete filling of interstices during deposition
- Presence of un-melted particles in the spray
- Satellite droplets formed by splat break-up at the time of impact
- Overshooting of liquid over solidified splats during droplet spreading
- Entrapment of gas between splats and the presence of an oxide layer on the spray particles.

Precursor powder can also be trapped by the molten splats. It should be noted that not all powder particles are fully molten when they land on the substrate. Some of them may be molten droplets without enough kinetic energy to form splats. The ceramic coating has chemical and structural uniformity to ensure reliable properties of coating such as low porosity and high dense structure. In addition to that, alumina powder can be sprayed using plasma process to produce high quality, high deposition efficiency and homogeneous coatings [21].

3.3. Coating thickness:

Fig.1(a−d) shows that coating thickness obtained from plasma spray of Al_2O_3 was larger than that WC−12%Co. Also the parallel coating direction of both coating types exhibits high coating thickness compared with perpendicular direction. Furthermore, the fact that Al_2O_3 were chemically relatively inert compared with WC−12%Co. With increasing of coating thickness, the diffusion resistance to the electrolyte through the coating increased because the transport path was lengthened [16].

3.4. Corrosion test

Polarization curves of WC−12%Co coating specimens denoted by (A) for perpendicular coating and (A1) for parallel coating and uncoated specimens in 0.5 M H_2SO_4 solution are given in Fig. 4. A better protection was found for specimen (A1), which has parallel coating. Moreover, a significant shift of the anodic curves towards higher current values was observed for polarization curves of uncoated and perpendicular coating specimens (A). The results shown in Figs.5 & 6 indicate that the coating process greatly influenced the coating performance. As shown in Fig.5, specimen (A) had the highest corrosion rate (20.07 mm/year), even higher than uncoated one (15.8 mm/year). Specimen (A1) exhibited a higher polarization resistance and a lower corrosion rate (13.2 mm/year) than uncoated specimen. The corrosion potential of specimen (A1) (−113 mV) was shifted toward the noble direction compared with specimen (A) (−320 mV) and uncoated specimen (−276 mV) as illustrated in Fig. (4). Fig.7, on the other hand, shows the polarization curves of Al_2O_3 coating specimens denoted by (B) for perpendicular coating and (B1) for parallel coating and uncoated specimen. It was found that specimen (B1) shows a significant increase in corrosion resistance, as indicated in Figs. (8) & (9). Al_2O_3 coating showed the same behavior as in WC−12%Co coating process. In Fig.8, the corrosion rate of uncoated specimen (15.8 mm/year) is lower than specimen (B) (17.6 mm/year) and higher than specimen (B1) (3.5 mm/year). From Fig.9 the corrosion

potential of specimen (B1) (−40 mV) was shifted toward the noble direction compared with specimen (B) (−294 mV) and uncoated specimen (−276 mV). The polarization curves in Fig.10 illustrate the general trends observed for all test specimens. From Figs.(11)&(12), the results confirm that parallel coating exhibited a significantly better corrosion-resistant-ability than the other coatings by virtue of more noble corrosion potential; although all polarization curves were characterized by a very similar trend. The corrosion potential values of the parallel coated samples (less negative) were higher than values of the perpendicular coated samples (more negative), which is conclusive. It indicates that the parallel coating deposition technique's passive layer was strong and provided more corrosion resistance and protection than that of the perpendicular coating deposition technique, as illustrated in Fig.12. The improvement in corrosion resistance of parallel coatings may be attributed to the chemical stability of the coating layer, which acts as barriers for the corrosion process. The holes and gaps on the surface are thus reduced, and consequently prevent the corrosive pits from growing up [22]. The critical factors affecting the corrosion characteristics of coatings are identified as:

(1) Their quality (crystallinity, purity, and residual stress)

(2) Structure.

Corrosion resistance of coatings is a function of many factors, including coating porosity, physical properties of materials and presence of oxide films [23]. The porosity is characteristic of plasma sprayed coatings (PSC) and strongly affects their corrosion behaviors. Generally, the corrosion rate increases with increasing porosity in the coatings. The electrolyte infiltrates into the inner portion of the coating through the structural imperfections such as pores and cracks or pinholes existing in the coating and comes into contact with the deeper portion of the coating causing corrosion [24,25].

3.5. Microstructure of corroded specimens

The SEM/EDX micrograph of the surface morphology of the uncoated specimen after the corrosion test is given in Fig.13. The chemical composition elements of the substrate specimen which uncoated, have been identified using EDX analysis as shown in Fig.13. Apparently, the uncoated specimen and perpendicular coating specimens of WC−12%Co and Al_2O_3 denoted by (A) and (B) respectively suffered severe corrosion as shown in Fig.13 and Fig.14−a,b. On the other hand, Fig.15−a shows that parallel coating specimen WC−12%Co (A1) is more corrosion resistant than the perpendicular specimen. In addition, the parallel coating specimen of Al_2O_3 (B1) in Fig.15−b shows a very good corrosion resistant, which is attributed to the high dense coating surface with a minimum number of pores. Optimization of the parallel plasma-coatings-deposition having characteristics [of WC−12%Co and Al_2O_3 coatings], showed improvement in uniform corrosion resistance. The variation in the uniform corrosion performance of this deposition technique is linked to crack propagation paths. As shown in Figs. 14, 16 & 17, there are many micro pores, laminar splats and straight columnar grains [13]. SEM micrographs of WC−12%Co coatings, shown in Fig. 14, illustrate the presence of high percentage of corrosion on the surface coat layer. Besides, EDX analysis confirms the corrosion reaching the base. EDX analysis confirms the presence of lamella structure of Al_2O_3 as shown in Fig.17. None of the coating surface shows any element of the substrate.

Conclusions

The experimental results reported in this research indicate that the corrosion behavior is affected by the coating process along the following lines:-

1- Parallel coating exhibited better corrosion protection than the perpendicular coating.

2- Specimen of Parallel coating (B1) recorded a markedly the best corrosion resistance.
3- The defects in Al_2O_3 coating were relatively few compared to WC−12%Co coating, and hence, the corrosion resistance of the Al_2O_3 coating was superior to that of the WC−12%Co coating.
4- The corrosion potential was nobler in case of parallel coating.
5- According to the microstructures, pitting corrosion was observed in the parallel coated samples; while in the perpendicular coated samples, sever attack , pitting corrosion and abrasion were observed .

Acknowledgment

The author wishes to acknowledge Central Metallurgical Research & Development Institute for the help in running some of the experimental work.

References

[1] Wang Y, Jiang S, Wang MD, Wang SH, Xiao TD, Strutt PR. Abrasive wear characteristics of plasma sprayed nanostructured alumina/titania coatings. Wear 2000;237:176–85.

[2] Yan DR, He JN, Wu JJ, Qiu WQ, Ma J. The corrosion behavior of a plasma spraying Al2O3 ceramic coating in dilute HC1 solution. Surf Coat Technol 1997;89:191–5.

[3] Singh VP, Sil A, Jayaganthan R. A study on sliding and erosive wear behaviour of atmospheric plasma sprayed conventional and nanostructured alumina coatings. Mater Design 2011;32:584–91.

[4] Sarikaya O. Effect of the substrate temperature on properties of plasma sprayed Al_2O_3 coatings. Mater Design 2005;26:53–7.

[5] Afrasiabi A, Saremi M, Kobayashi A. A comparative study on hot corrosion resistance of three types of thermal barrier coatings: YSZ, YSZ+Al_2O_3 andYSZ/ Al_2O_3. Mater Sci Eng A 2008;478:264–9

[6] D. Thirumalai kumarasamy, K. Shanmugam1, V. Balasubramanian, " Corrosion performance of atmospheric plasma sprayed aluminacoatings on AZ31B magnesium alloy under immersion environment, " Journal of Asian Ceramic Societies 2014.

[7] Demirkiran, A.S., Celik, E., Yargan, M. and Avci, E. (2001). Oxidation Behaviour of Functionally Gradient Coatings Including Different Composition of Cermets, Surface and Coatings Tech., 142–144: 551–556.

[8] Soykan, S., Ustel, F., Celik, E. and Avci, E. (1997). Investigation of Friction and Wear Behaviours of Plasma Sprayed Ceramic Coating, Journal of Turkish Eng. and Environ. Sciences, 21: 417-423.

[9] Ashary A.A., Tucker R.C., Corrosion characteristics of several thermal spray cermet/coating alloy systems, Surface and Coatings Technology. 49, 1991, 78 – 82

[10] J. Munemasa, T. Kumakiri, "Effect of the surface roughness of substrates on the corrosion properties of films coated by physical vapour deposition" Surface and Coatings Technology 49 (1991) 496.

[11] B. Matthes, E. Broszeit, J. Aromaa, H. Ronkainen, S.-P. Hannula, A. Leyland, A. Mathews," Corrosion performance of some titanium-based hard coatings"Surface and Coatings Technology 49 (1991)489.

[12] F.S. Pettit," Summary Abstract: The requirements for developing corrosion resistant " Journal of Vacuum Science & Technology. A 4 (1986)3025.

[13] C.J. Li and A. Ohmori, Relationships Between the Microstructure and Properties of Thermally Sprayed Deposits, J. Therm. Spray Technol., 2002, 11(3), p 365-374

[14] I.Yu. Konyashin, T.V. Chukalovskaya, A technique for measurement of porosity in protective coatings, Surface and Coatings Technology, 88 (1996), pp. 5–11

[15] C.S.Ramachandran,V.Balasubramanian and P. Ananthapadmanabhan, Multiobjective optimization of atmospheric plasma spray process parameters to deposit yttria-stabilized zirconia coatings using response surface methodology, J. Therm. Spray. Technol. 20 (2010), 590-607.

[16] Zhe Liu , Yanchun Dong, Zhenhua Chu, Yong Yang, Yingzhen Li, Dianran Yan ," Corrosion behavior of plasma sprayed ceramic and metallic coatings on carbon steel in simulated seawater," Materials and Design 52 (2013) 630–637

[17] G. Antou, G. Montavon, F. Hlawka, A. Cornet and C. Coddet, "Characterizations of the pore-crack network architecture of thermal-sprayed coatings "Mater. Charact., 53,361–372 (2004).

[18] N. Ahmed, M.S. Bakare, D.G. Mccartney, and K.T. Voisey, The Effects of Microstructural Features on the Performance Gap in Corrosion Resistance between Bulk and Hvof Sprayed Inconel 625, Surf. Coat. Technol., 2010, 204(14), p. 2294-2301

[19] Roge, B., Fahr, A., Giguere, J. S. R. and Mcare, K. I., 'Nondestructive Measurement of Porosity in Thermal Barrier Coatings', Journal of Thermal Spray Technology, Vol. 12, No. 4, pp. 530-535, 2003

[20] Gudmundsson, B., Jacobson, B. E., Berglin, L., Lestrade, L., and Gruner, H., "Microstructure and Erosion Resistance of Vacuum Plasma Sprayed Co-Ni-Al-Y/Al_2O_3 **Composite** Coatings", 1st Plasma Technik Symposium, Lucerne, Switzerland, Vol. 2, May 1988, PP.105-114.

[21] Ding, C., Lin, H., Qu, J., Zhang, Y., and Zhang, H.,"Chromia and Alumina Titania Oxide Ceramic Powder For Plasma Spraying", 1st Plasma Technik Symposium, Lucerne, Switzerland, Vol. 2, May 1988, PP.221-228.

[22] Morks Magdi, Fahim Narges and Kobayshi. " Microstructural, corrosion behavior and microhardness of plasma sprayed W-Ni composite coatings" Transactions of JWRI,vol.36,2007,45-50

[23] Roman, O.V., ILyuschenko, A. Ph., Verstak, A. A., and Nekrashevich, M. S., " Evaluation of Wear Resistance of APS and VPS Metal Carbide/Metal Coating Systems",1st Plasma Technik Symposium, Lucerne, Switzerland, Vol. 2, May 1988, PP.15-24.

[24] E. Celik, I. Ozdemir, E. Avci and Y. Tsunekawa. “Corrosion behaviour of plasma sprayed coatings” Surface and Coatings Technology, Vol. 193, n 1-3., Apr 1, 2005, PP. 297-302,

[25] Chun-Cheng Chen1 and Shinn-Jyh Ding.“Effect of Heat Treatment on Characteristics of Plasma Sprayed Hydroxyapatite Coatings” Materials Transactions, Vol. 47, No. 3 (2006) pp. 935 to 940.

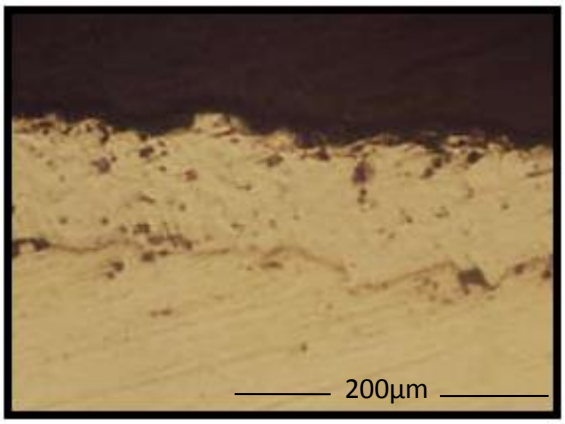

(a): A1 (minimum porosity)

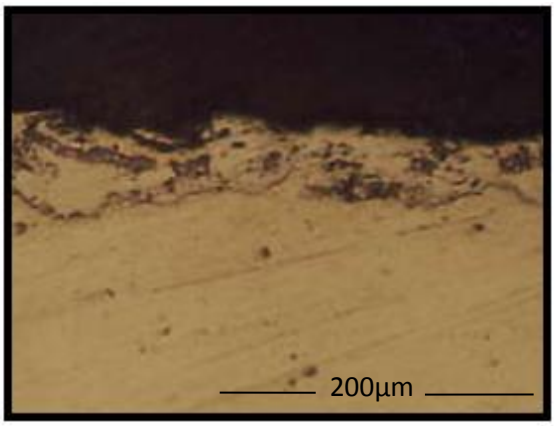

(b): A (more porosity)

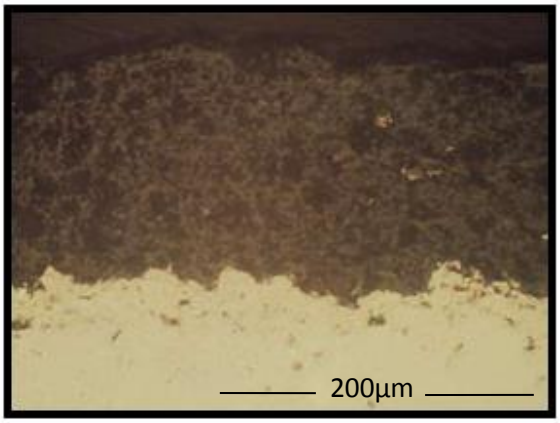

(c) :B1 (very small porosity)

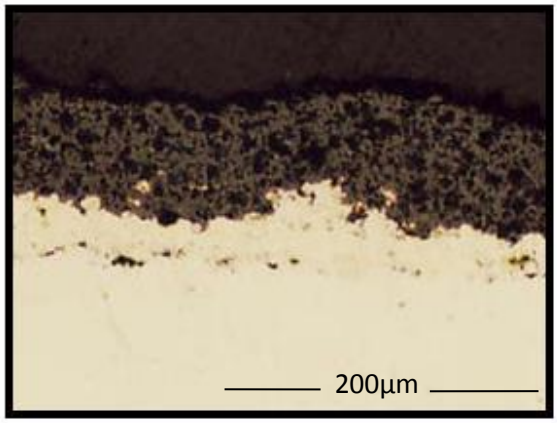

(d): B (more and bigger porosity)

Fig.1. Microstructures of coating specimens 500X.

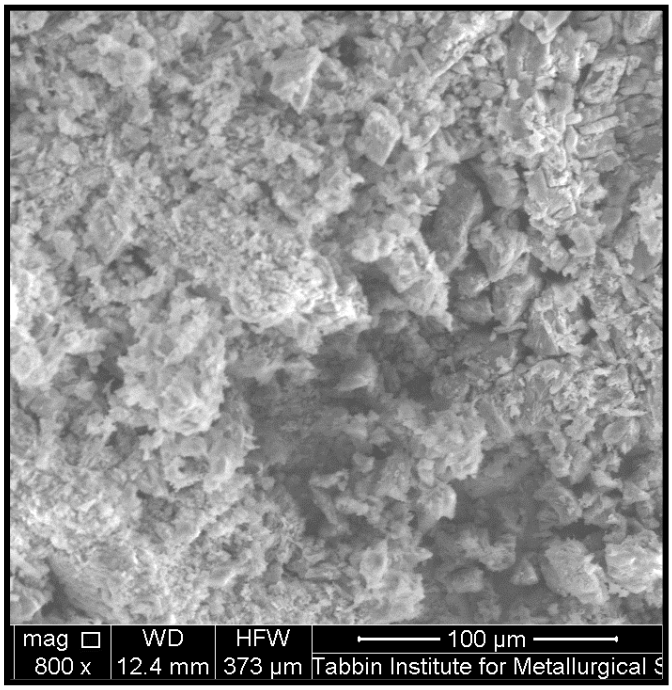

Fig.2. SEM micrograph of WC−12%Co coating

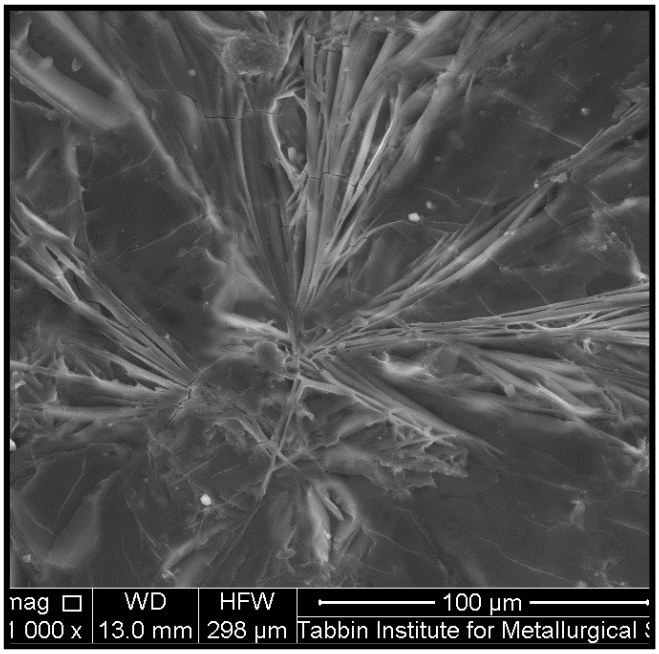

Fig.3. SEM micrograph of Al_2O_3 coating

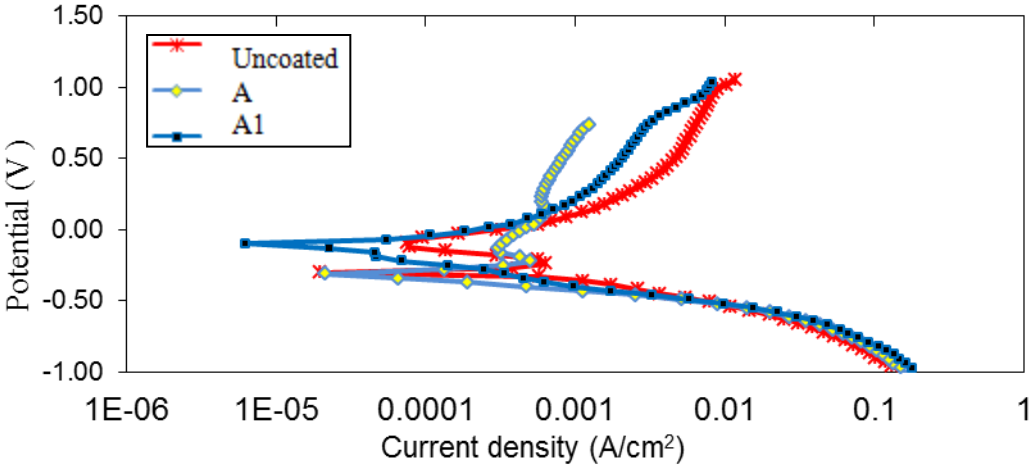

Fig.4. Potentiodynamic polarization curves for samples coated by WC-12%Co in 0.5 M H_2SO_4

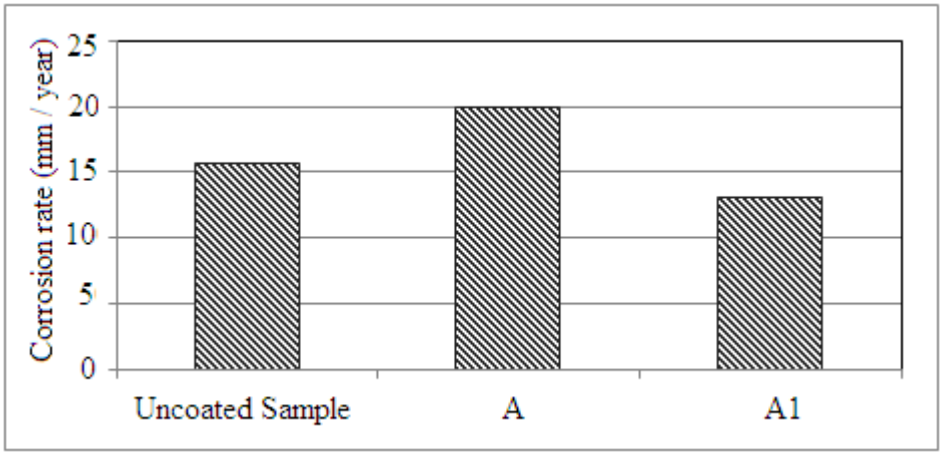

Fig.5. Corrosion rate of samples coated by WC-12%Co in 0.5 M H_2SO_4

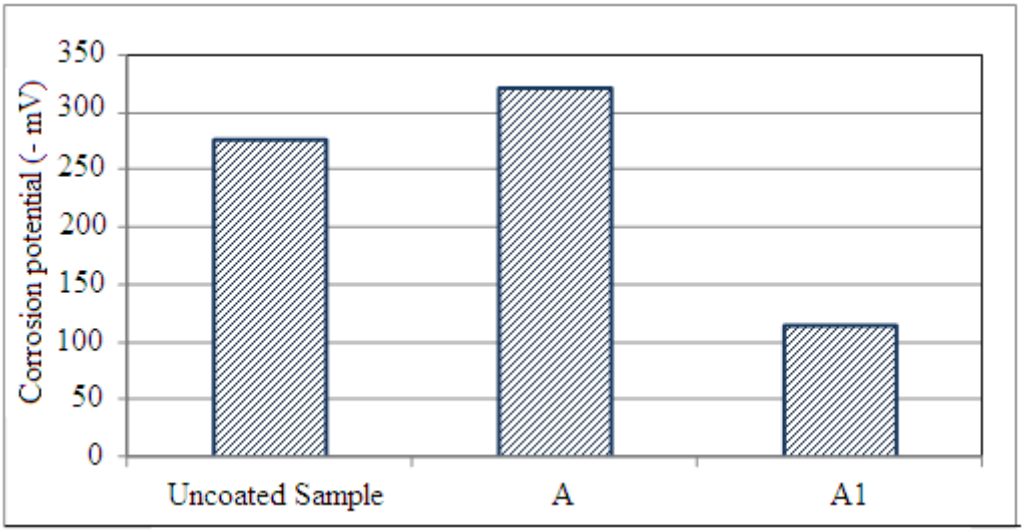

Fig.6. Corrosion potential of samples coated by WC-12%Co in 0.5 M H_2SO_4

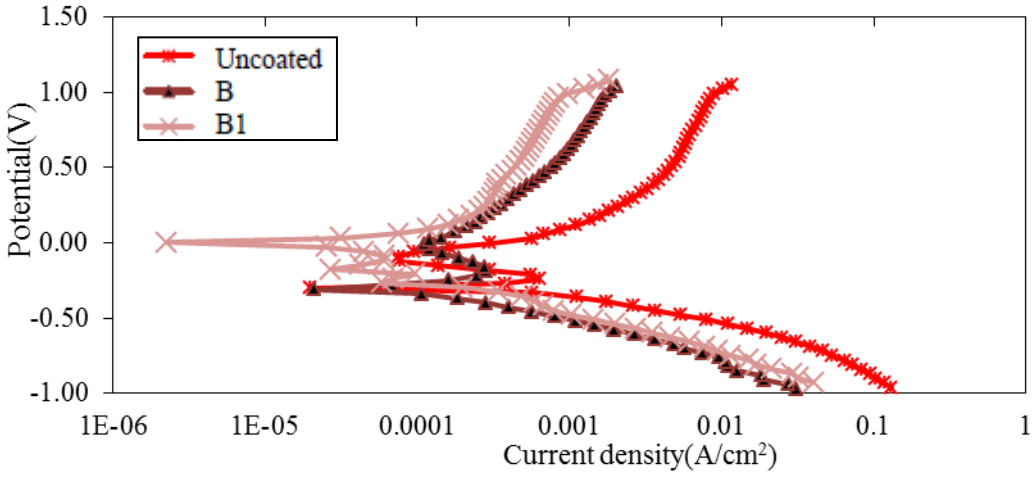

Fig.7. Potentiodynamic polarization curves for samples coated by Al_2O_3 in 0.5 M H_2SO_4

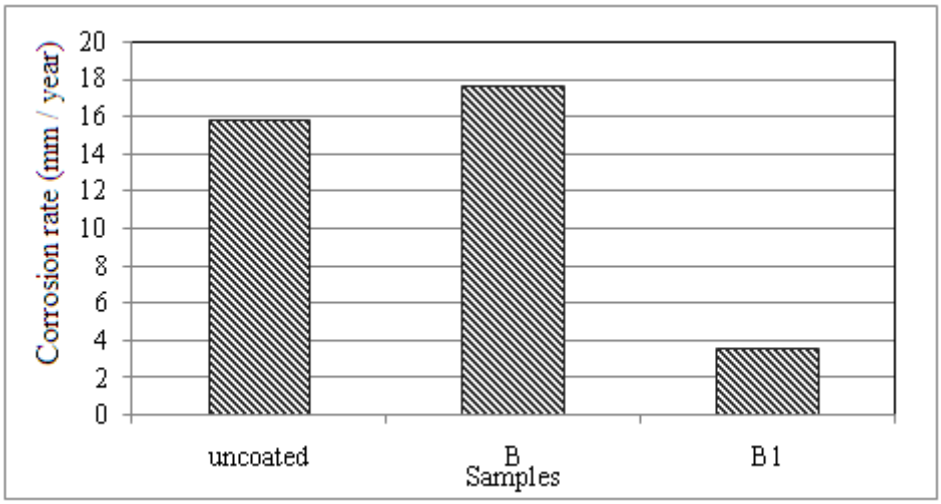

Fig.8. Corrosion rate of samples coated by Al_2O_3 in 0.5 M H_2SO_4

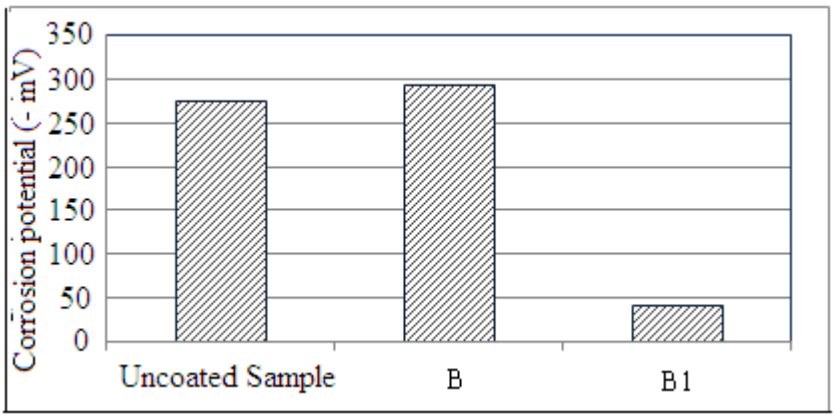

Fig.9. Corrosion potential of samples coated by Al_2O_3 in 0.5 M H_2SO_4

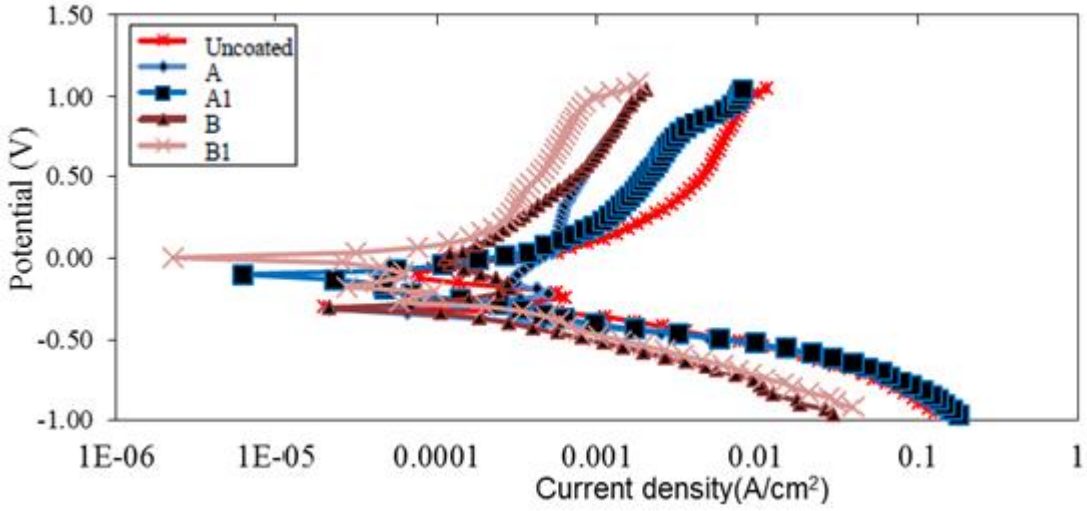

Fig.10. Potentiodynamic polarization curves for coated samples in 0.5 M H_2SO_4

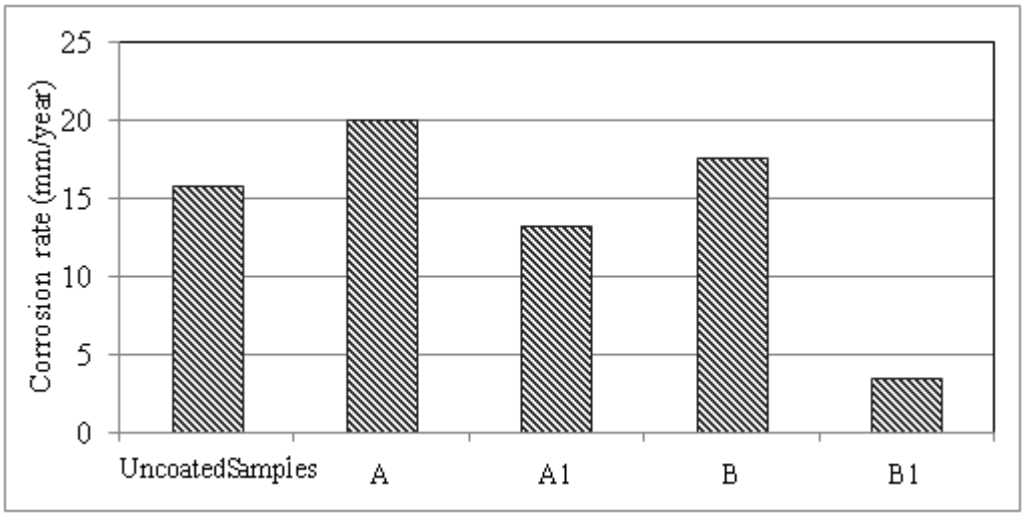

Fig.11. Corrosion rate of coated samples

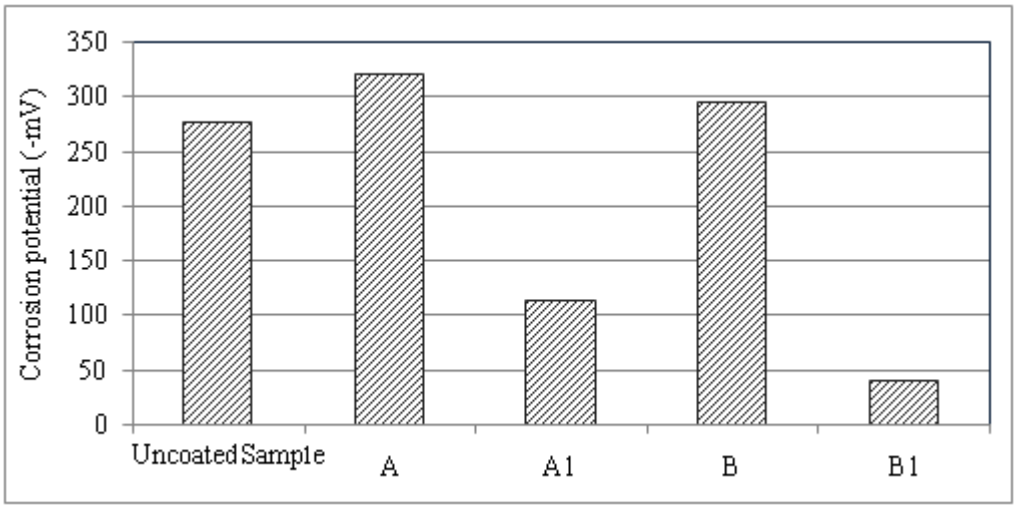

Fig.12. Corrosion potential of coated samples.

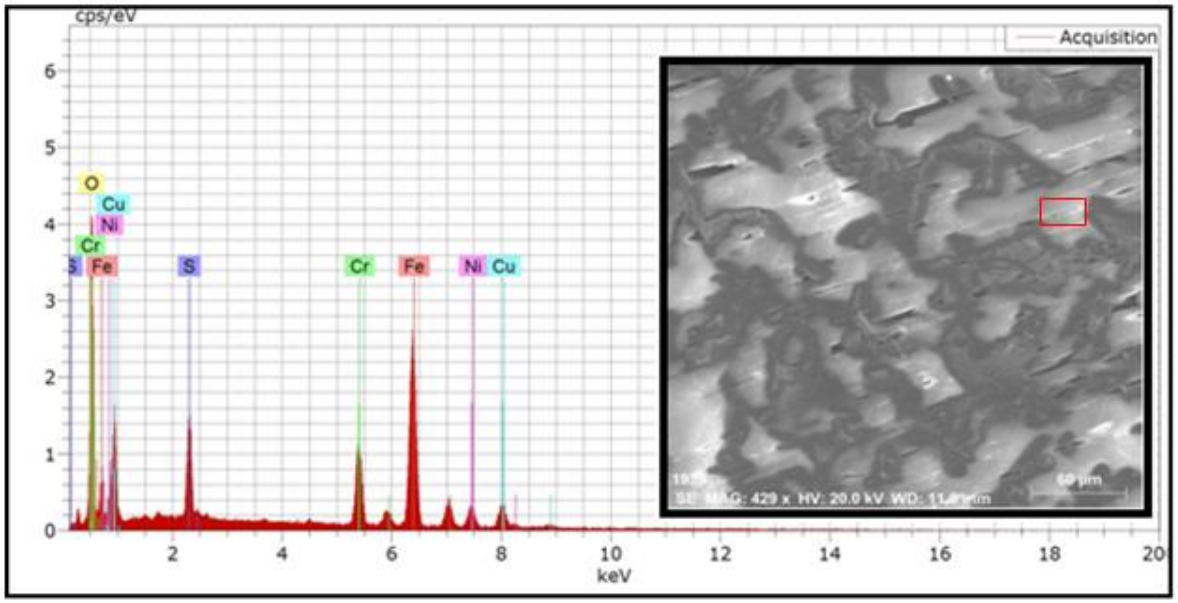

Fig.13. EDX corroded surface of uncoated specimen 1000X

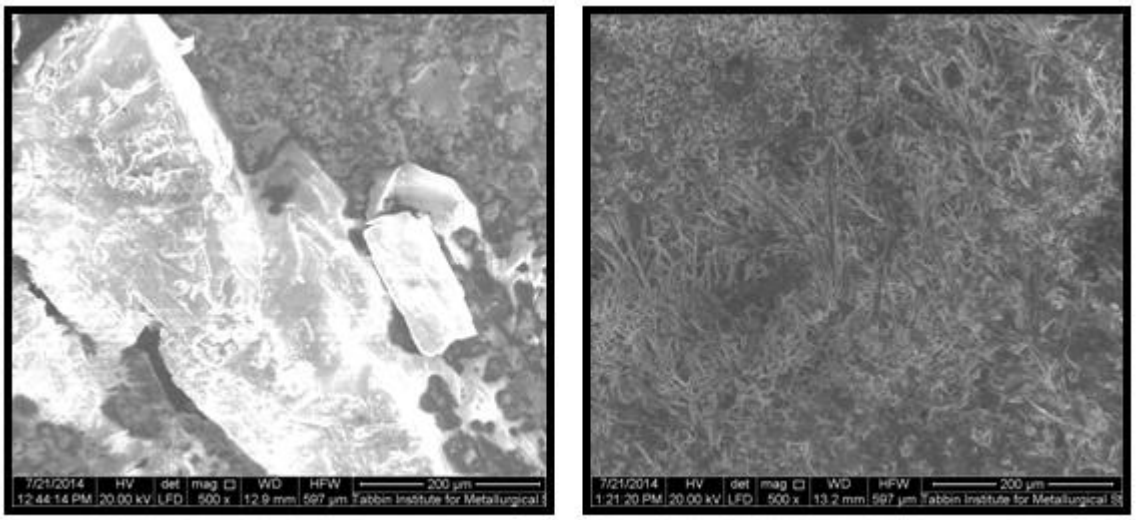

a:SEM of (A) 500X (Severe corrosion attack)

b: SEM of (B) 500X (Columnar grains)

Fig.14. SEM micrographs of perpendicular coating specimens of WC-12% Co and Al_2O_3

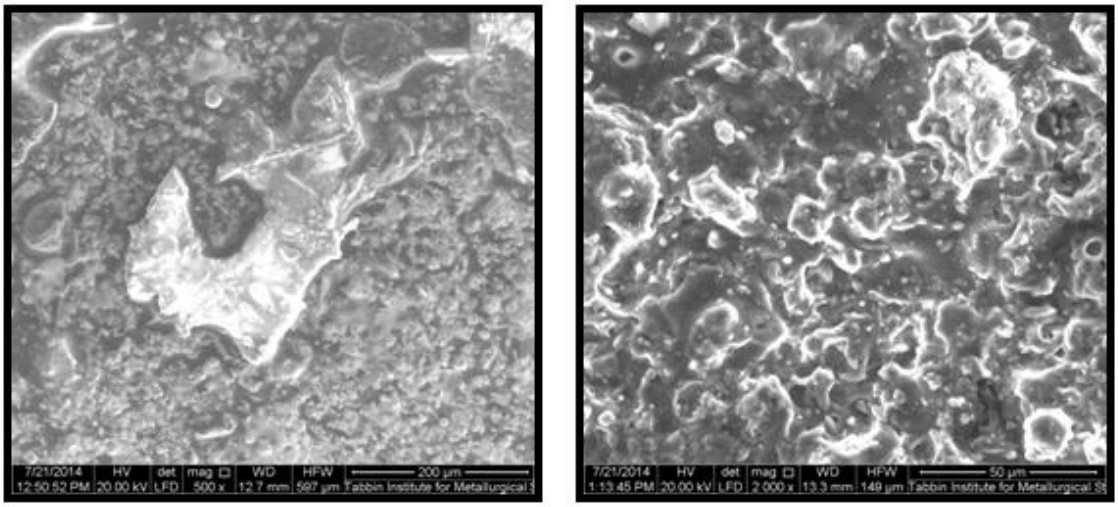

a:SEM of (A1) 500X b:SEM of (B1) 500X

Fig.15. SEM micrographs of parallel coating specimens of WC-12% Co and Al_2O_3

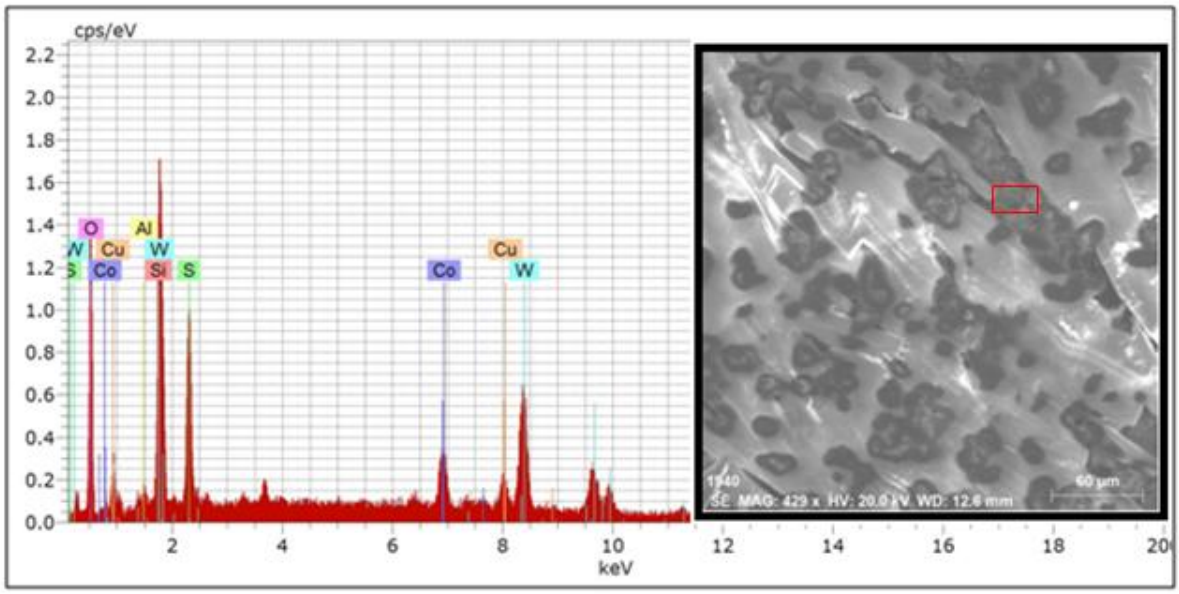

Fig.16. EDX analysis of specimen (A) and SEM of coating specimen (A) WC-12% Co ⊥ 1000X

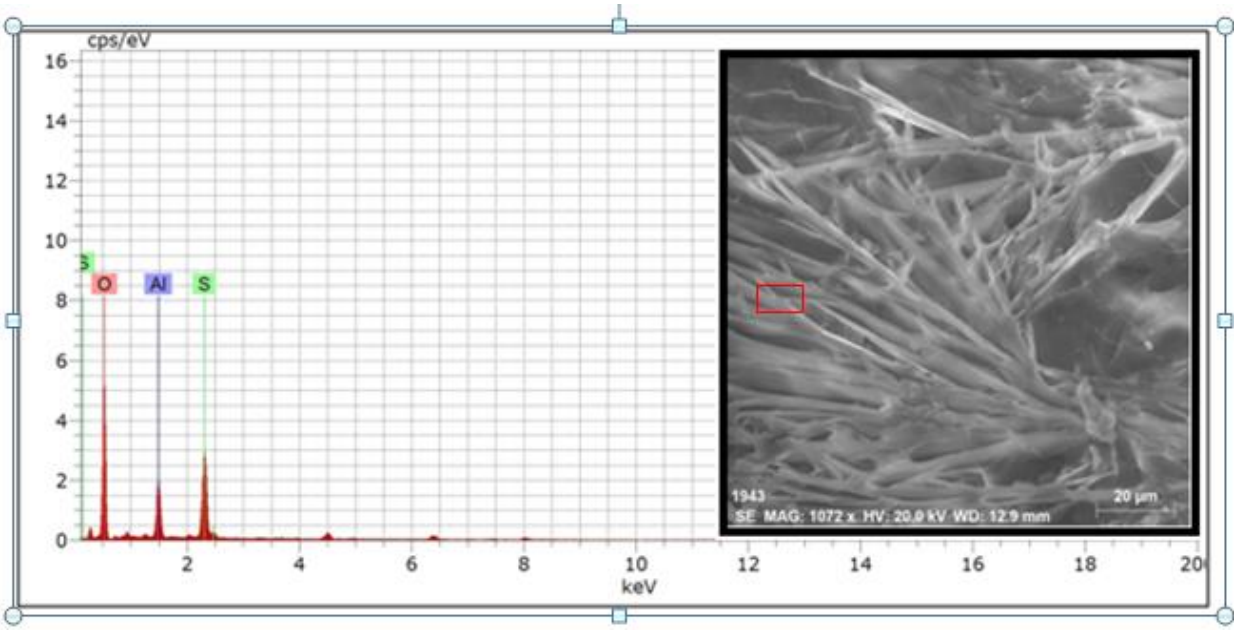

Fig.17. EDX analysis of (B) and SEM of coating specimen (B) (Laminar grains)

$Al_2O_3 \perp$ 1000X

Table 1. Spray parameters for plasma burner PT F4-HB / F4-MB:

Spray parameters	Unit	Gray Aluminum Oxide Powder (Al_2O_3)	Tungsten Carbide- Cobalt (WC-12%Co)
Plasma gases		Ar / H_2	Ar / He
Amperage	A	500	820
Voltage	V	70- 72	57-60
Plasma gas flow	SLPM	47/ Ar and 12/ H_2	74/Ar and 122/ He
Powder flow	g/min	30	30
Carrier gas flow	SLPM	2.5	2.6
Anode diameter	mm	normal	6 (inside)
Spray distance	mm	100	125 - 130
Powder injector	mm	1.8	2
Cooling		air	Air or CO_2

Table 2. The porosity results of ceramic plasma spray coatings

Coating specimens	**B1**	**A1**	**B**	**A**
Porosity %	7	9	12	17
Corrosion rate (mm/year)	3.5	13.2	17.6	20.07